

Characterization of supported lipid bilayers incorporating the phosphoinositides phosphatidylinositol 4,5-bisphosphate and phosphoinositol-3,4,5-triphosphate by complementary techniques

Martina K. Baumann, Esther Amstad, Alireza Mashaghi, Marcus Textor, and Erik Reimhult^{a)}

Laboratory for Surface Science and Technology (LSST), Department of Materials, ETH Zurich, Wolfgang-Pauli-Strasse 10, CH-8093 Zurich, Switzerland

(Received 16 July 2010; accepted 15 October 2010; published 15 November 2010)

Phosphoinositides are involved in a large number of processes in cells and it is very demanding to study individual protein-lipid interactions *in vivo* due to their rapid turnover and involvement in simultaneous events. Supported lipid bilayers (SLBs) containing controlled amounts of phosphoinositides provide a defined model system where important specific recognition events involving phosphoinositides can be systematically investigated using surface sensitive analytical techniques. The authors have demonstrated the formation and characterized the assembly kinetics of SLBs incorporating phosphatidylinositol 4,5-bisphosphate (PIP₂; 1, 5, and 10 wt %) and phosphoinositol-3,4,5-triphosphate (1 wt %) using the quartz crystal microbalance with dissipation monitoring and fluorescence recovery after photobleaching. An increased fraction of phosphoinositides led to a higher barrier to liposome fusion, but full fluidity for the phosphatidylcholine lipids in the formed SLB. Significantly, the majority of phosphoinositides were shown to be immobile. X-ray photoelectron spectroscopy was used for the first time to verify that the PIP₂ fraction of lipids in the SLB scales linearly with the amount mixed in from stock solutions. © 2010 American Vacuum Society. [DOI: 10.1116/1.3516485]

I. INTRODUCTION

Phosphatidylinositol (PtdIns) and its phosphorylated products, the phosphoinositides, play a special role among the phospholipids in mammalian cells. The PtdIns head group can be reversibly phosphorylated at the inositol ring at positions 3, 4, and 5 to yield seven different phosphoinositide species (Fig. 1). In contrast to PtdIns, phosphoinositides are only a minor species and occur in the cytoplasmic leaflet of cellular membranes, where they interact with a variety of different enzymes to perform fundamental regulatory functions.^{1,2} Phosphoinositides can also enact direct signaling by binding their head group to cytosolic proteins and cytosolic domains of membrane proteins. By this, they regulate the function of integral membrane proteins and recruit cytoskeletal and signaling components to the cell membranes.² In mammalian cells, phosphatidylinositol 4,5-bisphosphate (PIP₂) is the most common. Traditionally, it is thought to comprise only 0.5%–1.0% of all phospholipid molecules in normal cells,^{3,4} although recent research indicates up to five times higher values.⁵

It is very difficult to specifically study the exclusive interactions of single protein domains with one lipid species *in vivo* due to the high turnover of both interaction partners and the molecular complexity of native membranes and cytosol composition. An *in vitro* platform, where the lipid composition of the membrane as well as the bulk solution composition can be precisely regulated, presents an excellent model system to study the binding affinities and kinetics of specific

protein domains to the lipid head group, in particular, for low abundance lipids such as phosphoinositides, which have rapid spatial and temporal regulations and turnover *in vivo*.^{1,6} In previous work, protein domain affinity to lipids has most commonly been studied using assays with bulk suspended liposomes as the model system for membranes.^{7–12} Surface sensitive techniques allow for a more direct and detailed detection in a time resolved manner of adsorption of molecules onto a membrane mimic physisorbed on the sensor surface. The control over and characterization of assembly of surface supported lipid bilayers (SLBs) from liposomes for biosensing has been a hot topic in biointerface science for more than a decade thanks to its high potential for many applications.^{13–16} Membrane conformation,¹⁷ lipid order,¹⁸ structure,¹⁹ mechanical²⁰ and electrical^{21,22} properties, and binding and insertion of peptides^{23–25} have all been probed using SLBs. For these reasons, Steinem and co-workers made use of SLBs incorporating PIP₂ to study specific interactions with ezrin using quartz crystal microbalance, scanning force microscopy, epifluorescence, and colloidal probe microscopy.^{26,27} However, they did not address or describe the formation and characterization of the PIP₂ SLB model system, which is crucial in extending PIP₂ SLBs as model system for further investigations. Especially, the quality of the formed SLB and the accessibility and mobility of incorporated PIP_x lipids are crucial for the interpretation of interaction measurements. Many phosphoinositide interactions have low affinity, and hence, multivalent binding and low background noise become important considerations.

In this work, we address in detail the formation and characterization of SLBs doped with PIP₂ and phosphoinositol-

^{a)}Electronic mail: erik.reimhult@mat.ethz.ch

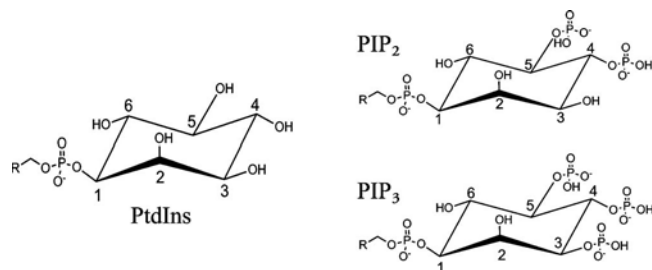


FIG. 1. PtdIns head group can be reversibly phosphorylated at the inositol ring at positions 3, 4, and 5 to yield seven different phosphoinositide species. In this work, we characterized SLB formation from POPC liposomes doped with PIP₂ and PIP₃.

3,4,5-trisphosphate (PIP₃) formed by liposome fusion on SiO₂ substrates for use with surface sensitive analytical techniques. PIP₂ and the less abundant PIP₃ were chosen for their different phosphorylation states as well as for their specific interaction with protein domains and their physiological convertibility by phosphatase and tensin homolog phosphorylase and phosphoinositide-3 kinase, which both act on the 3' phosphate on the inositol ring.^{2,5,28,29} The investigated phosphoinositide concentration range in the lipid mixtures was selected to yield a good surface coverage close to the physiologically relevant range,²⁶ with the aim to present enough binding sites to study protein interactions and measure detailed binding kinetics. The kinetics of SLB self-assembly from liposomes was characterized using quartz crystal microbalance with dissipation monitoring (QCM-D). Fluorescence recovery after photobleaching (FRAP) was used to further characterize lipid mobility and quality of the formed SLB, whereas x-ray photoelectron spectroscopy (XPS) was used for the first time to prove that the incorporation of PIP₂ into the supported lipid bilayer linearly scales with the amount of PIP₂ added to liposomes.

II. RESULTS AND DISCUSSION

To form SLBs on the substrates, we used the method pioneered by McConnell *et al.*³⁰ In brief, the SiO₂ substrates were exposed to lipid vesicle solutions (for a detailed experimental description, see Ref. 31). Liposomes were prepared from lipids mixed to the desired composition in CHCl₃. After evaporation of the CHCl₃ under steady N₂ flow for 1 h, the lipid film was rehydrated with tris buffered saline (TBS, 10 mM tris(hydroxymethyl)aminomethane, 150 mM NaCl, pH 7.4 by 2 mM HCl) to a final lipid concentration of 0.5 mg/ml. After solubilization in the buffer at room temperature, the lipid mixture was extruded 31 times through two stacked polycarbonate membranes (pore size 100 nm, Avestin, Canada). QCM-D experiments were performed at 37 °C on a QCM-D E4 (Q-Sense AB, Sweden).³² Upon surface contact, the liposomes adsorb and rupture to form a continuous SLB after a critical surface coverage has been reached.³³ QCM-D allows time resolved detection and monitoring of the SLB formation on the crystal surface.

In a first approach to form SLBs, we tried to use TBS supplemented with 2 mM Ca²⁺ to enhance surface interactions, which has been demonstrated to promote SLB formation for negatively charged liposomes containing phosphatidylserine (PS) lipids by Rossetti *et al.*³⁴ However, these buffer conditions did not result in successful SLB formation on SiO₂ coated crystals (see Fig. 1 of Ref. 31). Carvalho *et al.* showed that Ca²⁺ concentrations of ~30 μM can induce clustering of PIP₂ in giant unilamellar vesicles.³⁵ Clustering of PIP₂ lipids in the vesicles could be a reason for the impeded SLB formation in the presence of Ca²⁺, and this hypothesis was tested by attempting SLB formation in TBS without Ca²⁺.

Phosphatidylcholine (POPC) bilayers with 1, 5, and 10 wt % PIP₂ incorporated were indeed formed in TBS [Fig. 2(A)]. The typical phases of vesicle adsorption up to a critical coverage (1), rupture (2), lateral fusion and formation of

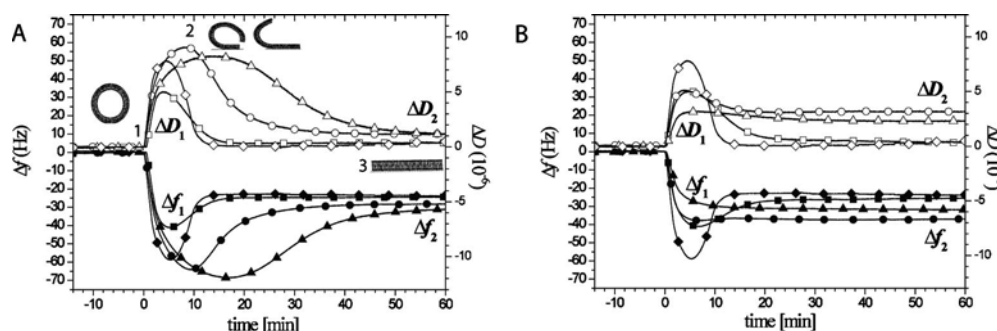


FIG. 2. (A) PIP₂ bilayer formation was monitored by QCM-D on SiO₂ crystals at 37 °C in TBS. Changes in dissipation (ΔD , open symbols) and frequency (Δf , filled symbols) correspond to typical kinetics of vesicle injection (1) and adsorption onto the SiO₂ crystal surface, followed by vesicle rupture (2) and supported lipid bilayer formation (3). ΔD and Δf of the representative fifth overtone are presented. Legend: ■ 1% PIP₂ (POPC: PIP₂ [99:1]), ● 5% PIP₂ (POPC: PIP₂ [95:5]), ▲ 10% PIP₂ (POPC: PIP₂ [90:10]), and ◆ POPC (pure) B. PIP₃ bilayer formation was monitored by QCM-D on SiO₂ crystals at 37 °C in TBS, pH 7.4. For vesicles with incorporated PIP₃ lipids, formation of bilayers was only observed for 1% PIP₃ content (square symbols). For higher PIP₃ fractions, the high remaining ΔD corresponds to only partial SLB formation and remaining intact vesicles on the sensor surface. ΔD and Δf of the representative fifth overtone are presented. Legend: ■ 1% PIP₃ (POPC: PIP₃ [99:1]), ● 2.5% PIP₃ (POPC: PIP₃ [97.5:2.5]), ▲ 5% PIP₃ (POPC: PIP₃ [95:5]), and ◆ POPC (pure).

the SLB (3) are indicated along the corresponding frequency (Δf) and dissipation (ΔD) shifts of the QCM-D measurements in Fig. 2(A). Longer adsorption and rupture times for SLB formation were measured for POPC vesicles doped with PIP₂ than for pure POPC vesicles. With PIP₂ fractions above 1%, the maximum frequency and dissipation shifts and time to reach the maximum upon vesicle adsorption as well as the final frequency shift measured for the SLB increased (see Table 1 of Ref. 31). The kinetics and final frequency and dissipation values ($\Delta D < 1$, Table 1 of Ref. 31) were in all cases associated with the formation of a SLB from negatively charged liposomes in close proximity to the substrate surface.³⁴

Vesicle deformation, which can be estimated from the $\Delta D/\Delta f$ ratio³⁶ (Fig. 2 and Fig. 2 of Ref. 31), as well as the adsorption rate (Fig. 2) were not significantly different for different amounts of incorporated PIP_x, and consequently, the surface interaction of the vesicles seems to be dominated by the POPC fraction. The latter is in good agreement with theoretical predictions by Dimitrievski and Kasemo,³⁷ who showed that the rapid diffusion of lipids within the liposome membrane leads to almost unperturbed adsorption kinetics for lipid compositions up to 50%/50% of zwitterionic and anionic lipids in their model. The surface induced deformation of the liposomes was decreased significantly in this model as the anionic lipid concentration was increased from 32% to 50%, which, however, is higher than the anionic lipid concentrations used in our experiments even after taking the high net charge of PIP_x lipids into account.

As observed directly in Fig. 2(A), the fusion and rupture of vesicles are significantly slowed down with increasing PIP₂ fractions, i.e., the critical surface coverage of vesicles before vesicle rupture (minimum in Δf and maximum in ΔD) was lower for vesicles incorporating 1% PIP₂ compared with vesicles incorporating 5% or 10% PIP₂. Therefore, the differences seen in higher coverage before the rupture of the vesicles seem to be due to a higher barrier to vesicle-vesicle fusion, to be overcome before the membrane proximity necessary for membrane fusion and rupture can be reached. Stronger electrostatic (or rather double layer) repulsion from the increased negative vesicle surface charge with increasing PIP₂ fraction is the likely origin of this increased barrier to close membrane proximity. Additionally, in a more molecular level model of the details of such an interaction including the effect of counter ions, if the initial adsorption of liposomes results in expulsion of PIP₂ from the adhesion zone with resultant redistribution of counter ion pairs on both sides of the lipid membrane, one can imagine an entropic mechanism as that described by Aranda-Espinosa *et al.*,³⁸ leading to a higher repulsive barrier to similarly charged objects through accumulation of charges on the membrane. With an increased entropic penalty for separating sufficient amount of PIP₂ charges from the liposome fusion zone with increasing total PIP₂ concentration, the kinetic barrier given by this intermediate state will further increase.

The apparent increased fusion and rupture barrier can also have a purely geometrical reason as the membrane potential

is decreased with increasing PIP₂ concentration. The vesicles are expected to adsorb at increasingly greater mean distance from each other as their surface charge density is increased, as has been observed, e.g., for colloidal particle surface adsorption as a function of screened electrostatic repulsion.³⁹ A greater mean distance would mean a higher surface concentration to bring the local surface concentration above the threshold level for strong membrane fusion and interaction, since the latter requires direct steric interaction of apposing membranes.

However, 1% PIP₂ containing liposomes ruptured at a lower coverage than pure POPC vesicles, which is counter to the trend observed above with increasing charge, leading to higher stability. We can only speculate on the reason for the significantly lower stability of PIP₂ containing liposomes relative to pure POPC liposomes. Dimitrievski and Kasemo³⁷ showed through simulations that the rapid adsorption and redistribution of liposomes with a large fraction of strongly surface adhering lipids can lead to the stabilization and early rupture of liposomes. One can assume that with a fraction of PIP₂ lipids, we have the reciprocal case of strongly repelled lipids in a membrane consisting mainly of moderately adhering lipids. The electrostatic interaction works in the opposite direction, but the effective outcome could be the same. In this scenario, due to their different charge and steric properties, the PIP₂ lipids could also locally destabilize the membrane by imposing a different local curvature and relatively long-range head group repulsion. For 1% PIP₂ vesicles, this reduction in vesicle stability from lipid flux during adsorption could be dominating over the effect of the relatively low surface charge density on the adsorption of close-by vesicles and membrane-membrane repulsive barrier, which will increase strongly as the membrane potential is decreased with increasing PIP₂ concentration.

As also observed by others, the formation of negatively charged membranes is not straightforward and the resulting membrane properties should be carefully characterized for each lipid composition.^{17,34,40} FRAP experiments were used to test the mobility of fluorescently labeled lipids in the SLB and to calculate the lipid diffusion coefficient, D . Fluorescently labeled vesicles were incubated on UV/Ozone cleaned glass cover slips (Menzel, Germany) and excess lipid solution was removed by exchange with pure TBS before fluorescence was bleached in a small area and the recovery of the fluorescence monitored (Table I and Fig. 3 of Ref. 31). The mobile fractions and diffusion constants were determined by the method of Jönsson *et al.*⁴¹ For 1%, 5%, and 10% PIP₂ with 1-palmitoyl-2-{12-[(7-nitro-2-1,3-benzoxadiazol-4-yl)amino]dodecanoyl}-*sn*-glycero-3-phosphocholine (NBD-PC), a high recovery of the fluorescence in the bleached area was observed, supporting the result from the QCM-D measurements of formation of a high quality SLB. FRAP experiments performed on PIP₂ SLB with TopFluor-labeled PIP₂ revealed a mobile fraction of only 30%–40%, indicating that most of the PIP₂ is immobile in the otherwise fluid SLB. A low mobile fraction of 20%–30% of PIP₂ in SLBs was also observed by Wagner and Tamm in incomplete

TABLE I. Mobile fractions and diffusion coefficients deduced by the method of Jönsson *et al.* (Ref. 41) from FRAP experiments for POPC bilayers containing increasing amounts of PIP₂ and PIP₃. In all experiments, 0.5% of labeled POPC and 0.1% of labeled PIP_x were used.

Bilayer composition	Mobile fraction (%)	Diffusion coefficient D ($\mu\text{m}^2/\text{s}$)
1% PIP ₂ , 99% *POPC (PC-NBD)	91.44 ± 4.54	2.44 ± 0.06
5% PIP ₂ , 95% *POPC (PC-NBD)	84.24 ± 1.63	2.46 ± 0.09
10% PIP ₂ , 90% *POPC (PC-NBD)	90.75 ± 1.52	1.84 ± 0.56
1% *PIP ₂ , 99% POPC (TopFluor-PIP ₂)	29.30 ± 4.93	2.09 ± 0.77
5% *PIP ₂ , 99% POPC (TopFluor-PIP ₂)	42.61 ± 4.78	3.14 ± 0.36
10% *PIP ₂ , 99% POPC (TopFluor-PIP ₂)	31.41 ± 5.44	2.79 ± 0.37
1% PIP ₃ , 99% *POPC (PC-NBD)	91.02 ± 2.02	2.16 ± 0.35
2.5% PIP ₃ , 97.5% *POPC (PC-NBD)	49.19 ± 4.85	1.43 ± 0.19
5% PIP ₃ , 95% *POPC (PC-NBD)	49.54 ± 4.86	1.79 ± 0.30
1% *PIP ₃ , 99% POPC (PIP ₃ -NBD)	13.64 ± 2.15	1.45 ± 0.74
2.5% *PIP ₃ , 97.5% POPC (PIP ₃ -NBD)	16.30 ± 4.63	1.09 ± 0.20
5% *PIP ₃ , 95% POPC (PIP ₃ -NBD)	28.65 ± 1.71	2.25 ± 0.32

planar bilayers supported on a tethered 3 mol % DMPE-polyethylene glycol (PEG)-triethoxy (DPS) PEG cushion with compositions dioleoyl phosphocholine:DPS (97:3)/POPC:PIP₂ (100–X:X) with X ranging from 0 to 5 mol % (with 1% NBD-PIP₂).^{42,43} The reasons for the low PIP₂ mobility are not yet determined. The negative charge of the large head group and steric demands thereof could play a role due to larger hydration shells and charge repulsion. Interaction with the underlying rough surface could lead to lower mobility of the PIP₂ in the proximal layer. An anionic head group could experience surface pits of similar dimensions in a negatively charged substrate as potential wells with repulsive walls if confined to move within the potential well, in analogy to what was recently shown for the trapping of nanoscale objects in such engineered wells in nanofluidic devices.⁴⁴ Thus, the high local negative charge and associated double layer could lead to repulsive trapping since, on a molecular length scale, the stiff membrane can provide the normal force to trap the lipid in the potential well. This is in contrast to trapping through attractive binding of the head group to the surface as was previously reported by, e.g., Rossetti *et al.* for Ca²⁺-mediated PS binding to TiO₂ substrates.³⁴ In the attractive case, all lipids flip and bind to the substrate surface.³⁴ We always observe a mobile fraction of close to half of all PIP₂ despite sufficient time for transbilayer lipid flip to occur during SLB formation.^{45,46} Rossetti *et al.* also documented by FRAP experiments that the distribution of PS is not affected by the negatively charged SiO₂ substrate surface in contrast to TiO₂ substrates.⁴⁰ A nonuniformly flat bilayer structure could also influence the fluidity. A self-organized curvature pattern could form driven by the differences in lipid dimensions between POPC and PIP_x lipids, especially in the head group region. Curved regions would be separated by flat areas hosting the immobile and mobile fractions of PIP_x, respectively. Obviously, any curved island will have a periphery with an opposite curvature sign (relatively lipid-free). This would lead to a compartmentalized

bilayer with impaired fluidity due to higher drag forces of the structured regions. ΔD shifts in the QCM-D measurements for successful SLB formation close to zero suggest that any such structure is below the nanometer scale and that the SLB is essentially macroscopically planar and in close proximity to the sensor surface as expected, making the verification of such roughness challenging. Clustering of PIP₂ lipids has been discussed repeatedly in literature, but was attributed to protein interaction with the membrane followed by rearrangement of the lipids. Fernandes *et al.* demonstrated that without such protein interactions, PIP₂ would not form domains in a POPC matrix in the pH range of 4.8–6.8.⁴⁷ However, for studies addressing the accessibility and concentration of binding sites as well as the final packing thereof, e.g., clustering studies, it is important to carefully assess the availability of mobile interaction partners at the SLB surface.

The diffusion coefficients found for the mobile fraction of TopFluor PIP₂ (2–3 $\mu\text{m}^2/\text{s}$) showed no strong dependence on the PIP₂ concentration and were similar to the POPC diffusion coefficients in the same membranes. These values approach the coefficients measured by Golebiewska *et al.* for giant unilamellar vesicles with PC and Bodipy-tetramethylrhodamine (TMR)-PIP₂ in PC/PS/PIP₂ ($D = 3.3 \pm 0.8 \mu\text{m}^2/\text{s}$) (Ref. 8) and are close to agreement with diffusion coefficients found for labeled Bodipy-TMR-PIP₂ in blebs formed on Rat1 cells ($D = 2.5 \pm 0.8 \mu\text{m}^2/\text{s}$).⁴⁸ The coefficients are distinctly higher than the coefficients found by Wagner and Tamm for NBD-PIP₂ (1% PIP₂: $D = 1.2 \pm 0.2 \mu\text{m}^2/\text{s}$, 5% PIP₂: $D = 0.85 \pm 0.15 \mu\text{m}^2/\text{s}$) and egg-phosphatidylethanolamine ($D = 0.6 \mu\text{m}^2/\text{s}$) in PEG-supported SLBs (Ref. 42) and are higher than the coefficients measured by Golebiewska *et al.* in the inner leaflet of native fibroblasts and epithelial cells for Bodipy-TMR-PIP₂ ($D = 0.8 \pm 0.2 \mu\text{m}^2/\text{s}$).⁴⁸

Liposomes with 1%, 2.5%, and 5% PIP₃ were produced for SLB formation. Lower percentages of PIP₃ were incorporated to mimic the lower abundance of PIP₃ than PIP₂ in biological membranes and also to account for the fact that the higher charge per PIP₃ head group could hinder SLB formation. The expected QCM-D kinetics for liposome adsorption and SLB formation could only be observed for 1% PIP₃ containing liposomes [Fig. 2(B)]. At higher PIP₃ percentage, only small, monotonous changes in frequency and dissipation were observed, indicating a low adsorbed total mass. Since the ratio $-\Delta D/\Delta f$ is a good indicator of whether planar membrane patches (ratio close to zero) or liposomes (high ratio) are adsorbed, we can conclude from the obtained data that the highest PIP₃ concentration leads to adsorption of submonolayers of liposomes.³⁶ For 2.5 mol % PIP₃, the kinetic curve indicates partial rupture of adsorbed liposomes through a slight maximum in the dissipation shift, resulting in part of the surface covered by intact liposomes, part by SLB patches, and part bare. However, FRAP experiments with NBD-POPC confirmed a SLB with a mobile fraction of 91% (Table I and Fig. 3 of Ref. 31) for SLBs with 1% PIP₃, in agreement with the QCM-D data. SLBs incorporating 2.5% and 5% PIP₃ did not show full recovery and mobile

fractions around 50% were deduced, in agreement with the only partial SLB formation as observed with QCM-D. Experiments with NBD-labeled PIP₃ in 1% PIP₃ SLB revealed a mobile fraction of only 13%, indicating even lower mobility of the triphosphoinositide in the fluid POPC SLB than for the diphosphoinositide. In view of the PIP₂ liposome results, electrostatic repulsion between the vesicles may be a contributing reason for the lower total vesicle adsorption and no SLB formation at higher PIP₃ concentrations, although the overall charge of these lipid compositions was lower than or did not exceed much the charge for a 10% PIP₂ SLB. We can only speculate along the same lines as outlined for the PIP₂ concentration dependence for fusion above about the origin of this apparent difference between PIP₂ and PIP₃ liposome adsorption and fusion. The redistribution of PIP₃ lipids to form a depletion zone for surface adhesion could be more difficult because of the higher compartmentalization effect due to curvature and of the higher entropic penalty for the larger number of charges that have to be redistributed, which are expected for the bulkier and higher charged PIP₃ compared with PIP₂.

In the literature, it is always implicitly taken for granted that the lipid compositions mixed to form liposomes directly correlate with the composition in the SLB formed by liposome fusion. For lipid compositions where one or more species impede SLB formation as demonstrated above for the phosphoinositides, the possibility of heterogeneity in the liposome solution leading to a surface induced selection and different composition of the SLB should be considered. To further investigate the influence of the molar ratio of phosphoinositides to POPC in the formed SLBs relative that of the bulk liposomes, compositional analysis using XPS was performed. SLBs were fused from liposomes containing 0, 1, 5, and 10 wt % PIP₂, mixed with POPC on SiO₂ wafers, and subsequently dried. (Please note that 1, 5, and 10 wt % PIP₂ as referred to in the text correspond to 0.7, 3.5, and 7 mol % PIP₂.) The molar ratio of N:P, which equals 1 for pure POPC bilayers and decreases with increasing amounts of phosphoinositides incorporated in the SLBs, was measured with XPS. To account for phosphorus contaminations in the SiO₂ wafer surfaces, the fraction of phosphorus corresponding to a constant P:Si ratio measured on clean control SiO₂ wafers was first subtracted from the total measured phosphorus. The remaining P was assigned to P of phospholipids and taken to calculate the atomic ratio of N:P. The N:P ratio of POPC bilayers, which theoretically have a molar ratio of N/P=1, was used to normalize the resulting N/P ratios. Despite the large error bars that result from sample inhomogeneities caused by inhomogeneous drying of the SLBs on the scale of the XPS beam spot (approximately 300 μm), a near linear increase in PIP₂ concentration averages in the SLBs with increasing amounts of phosphoinositide added to the lipid film prior to liposome formation was evident (Fig. 3). Although the standard errors are large, the average measured PIP₂ concentrations are even higher than the mixed ratios, which indicates that the incorporation efficiency of PIP₂ into the SLBs (and thus supposedly also into the liposomes the

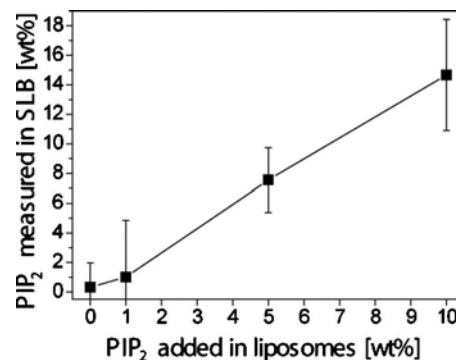


FIG. 3. wt % ratios of PIP₂ to POPC in SLBs scale linearly with the amount of mixed in phospholipids in the liposomes as measured with XPS. The molar ratios of N:P were analyzed to determine the amount of incorporated PIP₂ into the SLBs. The error bars [SEM with $n(\text{POPC})=6$, $n(1\% \text{ PIP}_2)=9$, $n(5\% \text{ PIP}_2)=7$, and $n(10\% \text{ PIP}_2)=6$] mainly result from inhomogeneities in the drying procedures prior to XPS analysis. Error bars for the PIP₂ concentrations expected mainly due to solvent evaporation from stock solutions and the use of measurement syringes were not included since they could not be quantified. A near linear increase in PIP₂ was observed.

SLBs are formed from) is at least expected within the investigated range of molar mixtures. Consequently, the SLB composition can be controlled by the lipid mixture in which the liposomes are formed from based on the mixed molar ratios.

III. CONCLUSION AND OUTLOOK

In summary, we have established negatively charged POPC SLBs on SiO₂ surfaces, incorporating physiologically relevant fractions of PIP₂ (up to 10 wt % PIP₂) and PIP₃ (up to 1 wt %) in tris buffer in the absence of calcium ions. Higher concentrations of PIP₃ did not result in complete SLB formation. After a SLB has been formed, the buffer can be easily exchanged also for a Ca²⁺ containing buffer. We could, for the first time, use XPS to verify that the molar ratio of POPC to PIP₂ in the SLBs scales consistently with the molar ratio used for liposome extrusion. The bilayer formation kinetics showed a dependence on the concentration of incorporated phosphoinositides (longer adsorption times for higher content). The same was true for the mobility of the lipid species in the SLBs (reduced mobility for PIP_x lipids compared with the POPC moieties). It was concluded that a higher fraction of PIP₂ mainly increased the barrier to liposome fusion. Adsorption of PIP₃ vesicles did not lead to SLB formation if more than 1% PIP₃ were incorporated and high concentrations even prevented significant liposome adsorption. Despite the low maximum concentration of 1% PIP₃ that could be incorporated into SLBs, it is still a physiologically relevant amount to study protein binding as PIP₃ also has a low abundance in biological membranes. For protein-lipid interaction studies, it is important to note that the mobility and the mobile fraction of the incorporated phosphoinositides might be altered compared to native cell membranes; therefore, special attention has to be paid in cases where mobility might play a role, e.g., for multivalent interactions or for determining maximum packing densities.

The presented, well characterized platform for phosphoinositide binding studies using surface sensitive analytical techniques enables real-time monitoring of detailed protein-lipid binding kinetics that goes beyond traditional dissociation constant determination, and thus, enables understanding of complex regulatory mechanisms such as coincidence detection of protein domains and multivalent binding.

ACKNOWLEDGMENTS

The authors thank the EU-FP7-NMP-ASMENA and the Swiss National Science Foundation, NCCR Project "Nano-scale Science" for research funding and acknowledge support from the Light Microscopy Center, ETH Zürich, LMC.

- ¹S. Corvera, A. D'Arrigo, and H. Stenmark, *Curr. Opin. Cell Biol.* **11**, 460 (1999).
- ²G. Di Paolo and P. De Camilli, *Nature (London)* **443**, 651 (2006).
- ³S. McLaughlin, J. Wang, A. Gambhir, and D. Murray, *Annu. Rev. Biophys. Biomol. Struct.* **31**, 151 (2002).
- ⁴A. Zachowski, *Biochem. J.* **294**, 1 (1993).
- ⁵D. Hilgemann, *Pfluegers Arch. Eur. J. Physiol.* **455**, 55 (2007).
- ⁶L. E. Hokin, *Annu. Rev. Biochem.* **54**, 205 (1985).
- ⁷N. A. Gokhale, A. Abraham, M. A. Digman, E. Gratton, and W. Cho, *J. Biol. Chem.* **280**, 42831 (2005).
- ⁸U. Golebiewska, A. Gambhir, G. Hangyás-Mihályiné, I. Zaitseva, J. Rädler, and S. McLaughlin, *Biophys. J.* **91**, 588 (2006).
- ⁹K. Krishnan, O. Holub, E. Gratton, A. H. A. Clayton, S. Cody, and P. D. J. Moens, *Biophys. J.* **96**, 5112 (2009).
- ¹⁰A. P. Liu and D. A. Fletcher, *Biophys. J.* **91**, 4064 (2006).
- ¹¹S. Takeda, A. Saitoh, M. Furuta, N. Satomi, A. Ishino, G. Nishida, H. Sudo, H. Hotani, and K. Takiguchi, *J. Mol. Biol.* **362**, 403 (2006).
- ¹²J. Tong, L. Nguyen, A. Vidal, S. A. Simon, J. H. P. Skene, and T. J. McIntosh, *Biophys. J.* **94**, 125 (2008).
- ¹³E. T. Castellana and P. S. Cremer, *Surf. Sci. Rep.* **61**, 429 (2006).
- ¹⁴E. Reimhult and K. Kumar, *Trends Biotechnol.* **26**, 82 (2008).
- ¹⁵R. P. Richter, R. Bérat, and A. R. Brisson, *Langmuir* **22**, 3497 (2006).
- ¹⁶M. Tanaka and E. Sackmann, *Nature (London)* **437**, 656 (2005).
- ¹⁷C. Merz, W. Knoll, M. Textor, and E. Reimhult, *BioInterphases* **3**, FA41 (2008).
- ¹⁸A. Mashaghi, M. Swann, J. Popplewell, M. Textor, and E. Reimhult, *Anal. Chem.* **80**, 3666 (2008).
- ¹⁹C. F. Majkrzak *et al.*, *Biophys. J.* **79**, 3330 (2000).
- ²⁰S. Kaufmann, G. Papastavrou, K. Kumar, M. Textor, and E. Reimhult, *Soft Matter* **5**, 2804 (2009).
- ²¹M. G. Friedrich, F. Gie, R. Naumann, W. Knoll, K. Ataka, J. Heberle, J. Hrabakova, D. H. Murgida, and P. Hildebrandt, *Chem. Commun. (Cambridge)* **2004**, 2376.
- ²²M. G. Friedrich, M. A. Plum, M. G. Santonicola, V. U. Kirste, W. Knoll, B. Ludwig, and R. L. C. Naumann, *Biophys. J.* **95**, 1500 (2008).
- ²³E. Briand, M. Zach, S. Svedhem, B. Kasemo, and S. Petronis, *Analyst (Cambridge, U.K.)* **135**, 343 (2010).
- ²⁴C.-W. Hsu, H.-R. Liou, W.-F. Su, and L. Wang, *J. Colloid Interface Sci.* **324**, 236 (2008).
- ²⁵N. Sanghera, M. J. Swann, G. Ronan, and T. J. T. Pinheiro, *Biomembranes* **1788**, 2245 (2009).
- ²⁶A. Herrig, M. Janke, J. Austermann, V. Gerke, A. Janshoff, and C. Steinem, *Biochemistry* **45**, 13025 (2006).
- ²⁷M. Janke, A. Herrig, J. Austermann, V. Gerke, C. Steinem, and A. Janshoff, *Biochemistry* **47**, 3762 (2008).
- ²⁸M. A. Lemmon, *Nat. Rev. Mol. Cell Biol.* **9**, 99 (2008).
- ²⁹S. McLaughlin and D. Murray, *Nature (London)* **438**, 605 (2005).
- ³⁰H. M. McConnell, T. H. Watts, R. M. Weis, and A. A. Brian, *Biochim. Biophys. Acta* **864**, 95 (1986).
- ³¹See supplementary material at <http://dx.doi.org/10.1116/1.3516485> for experimental protocol for vesicle preparation, QCM-D and FRAP experiments and additional data of SLB characterization as well as the sample preparation and normalization values used for the XPS analysis.
- ³²M. Rodahl, F. Hook, A. Krozer, P. Brzezinski, and B. Kasemo, *Rev. Sci. Instrum.* **66**, 3924 (1995).
- ³³E. Reimhult, M. Zach, F. Hook, and B. Kasemo, *Langmuir* **22**, 3313 (2006).
- ³⁴F. F. Rossetti, M. Bally, R. Michel, M. Textor, and I. Reviakine, *Langmuir* **21**, 6443 (2005).
- ³⁵K. Carvalho, L. Ramos, C. Roy, and C. Picart, *Biophys. J.* **95**, 4348 (2008).
- ³⁶E. Reimhult, F. Hook, and B. Kasemo, *J. Chem. Phys.* **117**, 7401 (2002).
- ³⁷K. Dimitrievski and B. Kasemo, *Langmuir* **24**, 4077 (2008).
- ³⁸H. Aranda-Espinoza, Y. Chen, N. Dan, T. C. Lubensky, P. Nelson, L. Ramos, and D. A. Weitz, *Science* **285**, 394 (1999).
- ³⁹P. Hanarp, D. S. Sutherland, J. Gold, and B. Kasemo, *J. Colloid Interface Sci.* **214**, 1 (2001).
- ⁴⁰F. F. Rossetti, M. Textor, and I. Reviakine, *Langmuir* **22**, 3467 (2006).
- ⁴¹P. Jönsson, M. P. Jonsson, J. O. Tegenfeldt, and F. Höök, *Biophys. J.* **95**, 5334 (2008).
- ⁴²M. L. Wagner and L. K. Tamm, *Biophys. J.* **81**, 266 (2001).
- ⁴³M. L. Wagner and L. K. Tamm, *Biophys. J.* **79**, 1400 (2000).
- ⁴⁴M. Krishnan, N. Mojarad, P. Kukura, and V. Sandoghdar, *Nature* **467**, 7316 (2010).
- ⁴⁵T. R. Khan, H. M. Grandin, A. Mashaghi, M. Textor, E. Reimhult, and I. Reviakine, *BioInterphases* **3**, FA90 (2008).
- ⁴⁶E. Reimhult, B. Kasemo, and F. Höök, *Int. J. Mol. Sci.* **10**, 1683 (2009).
- ⁴⁷F. Fernandes, L. M. S. Loura, A. Fedorov, and M. Prieto, *J. Lipid Res.* **47**, 1521 (2006).
- ⁴⁸U. Golebiewska, M. Nyako, W. Woturski, I. Zaitseva, and S. McLaughlin, *Mol. Biol. Cell* **19**, 1663 (2008).